

MZ-TH/00-07

hep-ph/0003115

March 2000

Threshold expansion of Feynman diagrams within a configuration space technique

S. Groote¹ and A.A. Pivovarov^{1,2}

¹ Institut für Physik, Johannes-Gutenberg-Universität,

Staudinger Weg 7, D-55099 Mainz, Germany

² Institute for Nuclear Research of the

Russian Academy of Sciences, Moscow 117312

Abstract

The near threshold expansion of generalized sunset-type (water melon) diagrams with arbitrary masses is constructed by using a configuration space technique. We present analytical expressions for the expansion of the spectral density near threshold and compare it with the exact expression obtained earlier using the method of the Hankel transform. We formulate a generalized threshold expansion with partial resummation of the small mass corrections for the strongly asymmetric case where one particle in the intermediate state is much lighter than the others.

1 Introduction

Perturbation theory remains the most accurate and reliable tool of theoretical analysis in elementary particle phenomenology. Even the most promising approach based on the direct calculation of physical observables on the lattice still cannot compete with perturbation theory supplemented with some non-perturbative additions as condensates or renormalons. The accuracy of experimental data for tests of the Standard Model permanently improves and demands the improvement of the accuracy of theoretical predictions [1]. Within perturbation theory this demand implies the calculation of Feynman diagrams with an increasing number of loops (see e.g. [2]). At present, Feynman diagrams of rather general form can be obtained analytically at most up to three loops. Any of these calculations is still unique and involves sophisticated algorithms and an extensive usage of computer resources (see e.g. [3, 4]). Even the notion of the analytical calculation is changing now because the analytical results are expressed through rather special transcendental numbers which eventually have to be calculated numerically. The striking example is the calculation of massive three-loop bubbles [4] where the analytical results for the diagrams are represented through the quantity which is given by a two-fold infinite sum (see also [5]). Not all of the multiloop Feynman diagrams are equally complicated. There are some topologies of n -loop diagrams or special kinematic regimes for the external momenta which are much simpler to compute than the general n -loop case (see e.g. [6]). The increasing complication of loop calculations within perturbation theory is more and more circumvented by using different kinds of expansion for the cases where the kinematics allows one to find a small parameter. Heavy Quark Effective Theory (HQET) and threshold expansions for heavy particle production are recent examples for such a situation. These expansions are mostly used for phenomenological applications where it even suffices to give approximate numerical values for the unexpanded multiloop integrals. In some cases one can obtain an analytical expansion that can be used for the simplification of the calculations or for the evaluation of the exact parameters of the effective

Lagrangians through matching conditions.

In this paper we discuss a method to calculate the near threshold expansion of the spectral density for the class of multiloop sunset-type Feynman diagrams termed water melon diagrams [7]. These diagrams has recently drawn some attention as a laboratory for testing some advanced methods in loop calculations [8, 9]. However, water melon diagrams also have numerous phenomenological applications. The most important application of these diagrams (as well as spectacle diagrams as their first generalization) is the calculation of the effective potential in quantum field theory both at finite temperature and at zero temperature [10, 11, 12, 13, 14, 15]. Among other applications one can name the sum rule analysis of baryons in QCD both in the massless approximation and with finite mass (the leading order correlator being the standard sunset diagram) [16, 17, 18, 19] or the treatment of baryons in the large N_c limit of QCD [20, 21] which requires the calculation of $(N_c - 1)$ -loop water melon diagrams in the leading order. An interesting application is the calculation of dibaryon properties in operator product expansion within the sum rule approach which is important for understanding many-quark bags in the nucleus [22, 23]. The water melon diagrams emerge in chiral perturbation theory [24, 25]. The corresponding integrals appear for the correlator of the effective operators related to the mixing of neutral mesons in flavour dynamics [26] and in the sum rule analysis of hybrid mesons [27]. Water melon diagrams constitute an important part of the contributions generated by the recurrence relations of the integration-by-part techniques for three-loop diagrams [28] (for the recent progress see e.g. Ref. [29]). It is a rather hot topic and a dynamically developing area of loop calculations where new results are frequently reported (see e.g. Refs. [30, 31, 32]).

In our opinion, the method presented in Ref. [7] completely solves the problem of computing this class of diagrams. The method is simple and reduces the calculation of a n -loop water melon diagram to a one-dimensional integral which includes only well-known special functions in the integrand (Bessel functions of different kinds) for any

values of the internal masses. The technique is universal. The most interesting part of our analysis of water melon diagrams is the construction of the spectral decomposition of water melon diagrams, i.e. the determination of the discontinuity across the physical cut in the complex plane of the squared momentum. In this context a novel technique for the direct construction of the spectral density of water melon diagrams based on an integral transform in configuration space was presented in Ref. [7]. In the present paper we develop some explicit expansions for water melon diagrams and compare them with the exact results. The purpose of this paper is a three-fold one, namely:

- to demonstrate the ease with which threshold expansions to arbitrary space-time dimensions and a general number of internal lines with arbitrary masses can be generated within a configuration space technique. The entire construction reduces to algebraic operations while the only integral encountered is a simple integral of the type of Euler's Gamma function.
- to generate explicit forms of threshold expansions and to analyze their convergence properties. The explicit forms of threshold expansions for the simple sunset can be compared with threshold expansions that are obtained in momentum space.
- to consider a case when one mass is much smaller than the others. This is an important generalization of the threshold expansion and can be analytically done within the configuration space technique.

The present analysis of the threshold expansion of water melon diagrams shows the effectiveness of the configuration space technique for this topology class of Feynman diagrams. On the other hand the obtained explicit results can be useful for a variety of applications which include the evaluation of water melon type diagrams. The technique can readily be generalized to some other simple topologies of n -loop diagrams.

The paper is organized as follows. In Sec. 2 we provide the tools necessary for the following calculations. Sec. 3 deals with the threshold expansion. Here we outline our

main strategy for this expansion in configuration space and in the subsections that follow we give examples for the sunset diagram and the water melon diagram with four or more internal lines. In Sec. 4 we concentrate on the strongly asymmetric case where one of the masses is much smaller than the others. We introduce the procedure of resummation of the contributions of this smallest mass and show explicitly how we get to a closed expression for the spectral density even in this case. We give examples for a strongly asymmetric mass arrangement for the water melon diagrams with two (degenerate case), three, and four or more internal lines, and compare the resummed results with the pure threshold expansion as well as with the exact spectral density. In Sec. 5 we discuss how to recover the non-analytic part of the polarization function through the spectral density near threshold. In Sec. 6 we give our conclusions.

2 Basics about the configuration space technique

We start with a brief outline of the technique which we use in this paper [7]. The polarization function $\Pi(x)$ of a water melon diagram including n internal lines with masses m_i , $i \in \{1, \dots, n\}$ in configuration space is given by the product

$$\Pi(x) = \prod_{i=1}^n D(x, m_i). \quad (1)$$

The propagator $D(x, m)$ of a massive line with mass m in D -dimensional (Euclidean) space-time is given by

$$D(x, m) = \frac{1}{(2\pi)^D} \int \frac{e^{ip_\mu x^\mu} d^D p}{p^2 + m^2} = \frac{(mx)^\lambda K_\lambda(mx)}{(2\pi)^{\lambda+1} x^{2\lambda}} \quad (2)$$

where we write $D = 2\lambda + 2$. $K_\lambda(z)$ is a McDonald function (a modified Bessel function of the third kind, see e.g. [33]). In the limit $m \rightarrow 0$ the propagator in Eq. (2) simplifies to

$$D(x, 0) = \frac{1}{(2\pi)^D} \int \frac{e^{ip_\mu x^\mu} d^D p}{p^2} = \frac{\Gamma(\lambda)}{4\pi^{\lambda+1} x^{2\lambda}} \quad (3)$$

where $\Gamma(\lambda)$ is Euler's Gamma function. Eq. (1) contains all information about the watermelon diagrams and in this sense is the final result for the class of diagrams under consideration. It is of course known and was used since long ago [34]. Of some particular interest is the spectral decomposition of the polarization function $\Pi(x)$ which is connected to the particle content of a given model. The spectrum of particles is contained in the function $\rho(s)$ related to the polarization function through the dispersion representation

$$\Pi(x) = \int_0^\infty \rho(s) D(x, \sqrt{s}) ds. \quad (4)$$

The dispersion representation of the polarization function in configuration space reveals the analytic structure of the polarization function $\Pi(x)$. For applications, however, one may need the Fourier transform of the polarization function $\Pi(x)$ given by

$$\Pi(q) = \int \Pi(x) e^{iq_\mu x^\mu} d^D x. \quad (5)$$

(We use the same notation for the function and its Fourier transform because we think that this will cause no confusion). Because of the Lorentz invariance of the propagator the angular integration in Eq. (5) can be done explicitly in D -dimensional space-time (for a generalization to tensor propagators see Ref. [7]). The result reads

$$\int e^{iq_\mu x^\mu} d^D \Omega = 2\pi^{\lambda+1} \left(\frac{|q||x|}{2} \right)^{-\lambda} J_\lambda(|q||x|) \quad (6)$$

where $J_\lambda(z)$ is the usual Bessel function and $d^D \Omega$ is the rotationally invariant measure on the unit sphere in the D -dimensional (Euclidean) space-time. Note that the polarization function $\Pi(x)$ as well as its Fourier transform $\Pi(q)$ are only functions of the absolute value $|x|$ and $|q|$. The same is of course valid also for the other occurring functions. To simplify the notation we often write $x = |x|$ and $q = |q|$ for these absolute values.

Note that propagators of particles with non-zero spin in configuration space representation can be obtained from the scalar propagator by differentiation with respect to the space-time point x . This does not change the functional x -structure and causes only minor modification of the basic technique (for details see Ref. [7] and references therein).

Our final representation of the Fourier transform of a water melon diagram is given by the one-dimensional integral

$$\Pi(q) = 2\pi^{\lambda+1} \int_0^\infty \left(\frac{qx}{2}\right)^{-\lambda} J_\lambda(qx) \Pi(x) x^{2\lambda+1} dx \quad (7)$$

which is a special kind of integral transformation with a Bessel function as a kernel. This integral transformation is known as the Hankel transform [35, 36]. The representation given by Eq. (7) is quite universal regardless of whether tensor structures are added or particles with vanishing momenta are radiated from any of the internal lines. Note in this context that Bessel functions are objects well-studied during the last two centuries. They therefore can be added to the list of elementary functions.

Because the dispersion representation of the polarization function in configuration space (or the spectral density of the corresponding polarization operator) has the form given in Eq. (4), the analytic structure of the polarization function $\Pi(x)$ can be determined directly in configuration space without having to compute its Fourier transform first. The transformation in Eq. (4) turns out to be a particular example of the Hankel transform, namely the K -transform [35, 36]. As pointed out in Ref. [7], the inverse K -transform in this case is given by

$$\rho(s) = \frac{(2\pi)^\lambda}{i s^{\lambda/2}} \int_{c-i\infty}^{c+i\infty} I_\lambda(\zeta\sqrt{s}) \Pi(\zeta) \zeta^{\lambda+1} d\zeta \quad (8)$$

where $I_\lambda(z)$ is a modified Bessel function of the first kind and the integration runs along a vertical contour in the complex plane to the right of the right-most singularity of $\Pi(\zeta)$. The inverse transform given by Eq. (8) completely solves the problem of determining the spectral density of the general class of water melon diagrams with any number of internal lines and different masses by reducing it to the computation of a one-dimensional integral. For n internal lines with equal masses m the spectral density reads explicitly

$$\rho(s) = \frac{m^{\lambda n}}{i(2\pi)^{(n-1)\lambda+n} s^{\lambda/2}} \int_{c-i\infty}^{c+i\infty} I_\lambda(\zeta\sqrt{s}) (K_\lambda(m\zeta))^n \zeta^{1-(n-1)\lambda} d\zeta. \quad (9)$$

In contrast to our technique, in the standard, or momentum, representation the polarization function $\Pi(q)$ is calculated from a $(n-1)$ -loop diagram with $(n-1)$ D -dimensional

integrations over the entangled loop momenta which makes the computation difficult when the number of internal lines becomes large.

3 Threshold expansion

With our method described in detail in Ref. [7] the s -dependence of the spectral density can be calculated by a one-fold numerical integration according to Eq. (8). The numerical integration in Eq. (8) can be done for arbitrary space-time dimensions and a general number of lines with arbitrary masses. In this sense this is the most efficient representation for the spectral density of the water melon diagram. However, we can also develop an explicit expansion near the threshold with any desired accuracy. It does not require any complicated integrations at all. The corresponding expansion of Eq. (8) can then be compared with series expansions near the production threshold obtained with the traditional momentum space technique. We stress that we are only interested in the spectral density because it is the main object for physical applications (see e.g. Refs. [37]). For practical reasons we start with Eq. (7). The polarization function $\Pi(q)$ as written in Eq. (7) is, in general, UV divergent. The divergence can be subtracted by using the power series expansion of the weight function $(qx/2)^{-\lambda} J_\lambda(qx)$ to an appropriate order which will be added and subtracted to this weight. This leads to a q^2 -dependent power series of divergent subtraction terms plus an UV finite subtracted integral (see e.g. [7, 38]). But because the subtraction terms do not contribute to the spectral density, we can avoid this subtraction at all. In order that the formally written expressions make sense they are supposed to be dimensionally regularized. We use the simplified or unorthodox dimensional regularization method for water melon diagrams (see Ref. [7]).

The threshold region of a water melon diagram is determined by the condition $q^2 + M^2 \simeq 0$ where q is the Euclidean momentum and $M = \sum_i m_i$ is the threshold value for the spectral density. We introduce the Minkowskian momentum p defined by $p^2 = -q^2$ which

is an analytic continuation to the physical cut. Operationally this analytic continuation can be performed by replacing $q \rightarrow ip$. To analyze the region near the threshold we use the parameter $\Delta = M - p$ which takes complex values. The parameter Δ is more convenient in Euclidean domain while the parameter $E = -\Delta = p - M$ is the actual energy counted from threshold which is used in phenomenological applications. The spectral density as a function of E is written as $\tilde{\rho}(E) = \rho((M+E)^2)$ in the following. The analytic continuation of the Fourier transform in Eq. (7) to the Minkowskian domain has the form

$$\Pi(p) = 2\pi^{\lambda+1} \int_0^\infty \left(\frac{ipx}{2}\right)^{-\lambda} J_\lambda(ipx) \Pi(x) x^{2\lambda+1} dx. \quad (10)$$

For the threshold expansion we have to analyze the large x behaviour of the integrand. It is this region that saturates the integral in the limit $p \rightarrow M$ or, equivalently, $E \rightarrow 0$. It is convenient to perform the analysis in a basis where the integrand has a simple large x behaviour. The most important part of the integrand is the Bessel function $J_\lambda(ipx)$ which, however, contains both rising and falling branches at large x . It resembles the situation with elementary trigonometric functions $\sin(z)$ and $\cos(z)$ to which the Bessel function $J_\lambda(z)$ is rather close (in a certain sense). Indeed, $\cos(z)$ (or $\sin(z)$) is a linear combination of exponentials, namely

$$\cos(z) = \frac{1}{2} (e^{iz} + e^{-iz}) \quad (11)$$

and has also both rising and falling branches at large pure imaginary argument: the exponentials show simple asymptotic behaviour $e^{\pm z}$ at $z = \pm i\infty$. The analogous statement is true for $J_\lambda(z)$ which can be written as a sum of two Hankel functions,

$$J_\lambda(z) = \frac{1}{2} (H_\lambda^+(z) + H_\lambda^-(z)) \quad (12)$$

where $H_\lambda^\pm(z) = J_\lambda(z) \pm iY_\lambda(z)$. The Hankel functions $H_\lambda^\pm(z)$ show simple asymptotic behaviour at infinity,

$$H_\lambda^\pm(iz) \sim z^{-1/2} e^{\pm z}. \quad (13)$$

Accordingly we split up $\Pi(p)$ into $\Pi(p) = \Pi^+(p) + \Pi^-(p)$ with

$$\Pi^\pm(p) = \pi^{\lambda+1} \int_0^\infty \left(\frac{ipx}{2}\right)^{-\lambda} H_\lambda^\pm(ipx) \Pi(x) x^{2\lambda+1} dx. \quad (14)$$

The two parts $\Pi^\pm(p)$ of the polarization function $\Pi(p)$ have completely different behaviour near threshold which allows one to analyze them independently. This observation makes the subsequent analysis straightforward. We first consider the contribution of the part $\Pi^+(p)$. The behaviour at large x is given by the asymptotic form of the functions which we simply write up to the leading terms as

$$H^+(ipx) = \sqrt{\frac{2}{i\pi px}} e^{-px} (1 + O(x^{-1})), \quad K(mx) = \sqrt{\frac{\pi}{2mx}} e^{-mx} (1 + O(x^{-1})). \quad (15)$$

The large x range of the integral (above a reasonably large cutoff parameter Λ) has the general form

$$\Pi_\Lambda^+(M - \Delta) \sim \int_\Lambda^\infty x^{-a} e^{-(2M-\Delta)x} dx \quad (16)$$

where

$$a = (n-1)(\lambda + 1/2). \quad (17)$$

The right hand side of Eq. (16) is an analytic function in Δ in the vicinity of $\Delta = 0$. It exhibits no cut or other singularities near the threshold and therefore does not contribute to the spectral density. We turn now to the second part $\Pi^-(p)$. In contrast to the previous case, the integrand of this part contains $H^-(ipx)$ which behaves like a rising exponential function at large x ,

$$H^-(ipx) \sim x^{-1/2} e^{px}. \quad (18)$$

Therefore the integral is represented by

$$\Pi_\Lambda^-(M - \Delta) \sim \int_\Lambda^\infty x^{-a} e^{-\Delta x} dx. \quad (19)$$

The function $\Pi^-(M - \Delta)$ is non-analytic near $\Delta = 0$ because for $\Delta < 0$ the integrand in Eq. (19) grows in the large x region and the integral diverges at the upper limit. Therefore the function which is determined by this integral is singular at $\Delta < 0$ ($E > 0$)

and requires an interpretation for these values of the argument Δ . In the complex Δ plane with a cut along the negative axis the function is analytic. This cut corresponds to the physical positive energy cut. The discontinuity across the cut gives rise to the non-vanishing spectral density of the diagram.

Let us first discuss the analytic part $\Pi^+(p)$ of the diagram. This part reduces to a regular water melon diagram. Indeed, using the relation

$$K_\lambda(z) = \frac{\pi i}{2} e^{i\lambda\pi/2} H_\lambda^+(iz) \quad (20)$$

between Bessel functions of different kinds one can replace the Hankel function $H_\lambda^+(ipx)$ with the McDonald function $K_\lambda(px)$. Since the propagator of a massive particle (massive line in the diagram) is given by the McDonald function up to a power in x , this substitution shows that the weight function behaves like a propagator of an additional line with the “mass” p . The explicit expression is given by

$$\Pi^+(p) = \frac{(-2\pi i)^{2\lambda+1}}{(p^2)^\lambda} \int_0^\infty \Pi_+(x) x^{2\lambda+1} dx. \quad (21)$$

$\Pi_+(x) = \Pi(x)D(x, p)$ is the polarization function of a new effective diagram which is equal to the initial polarization function multiplied by a propagator with p as mass parameter. We thus end up with a vacuum bubble of the water melon type with one additional line compared to the initial diagram (see Fig. 1). These diagrams have no singular behaviour at the production threshold $p = M$. As mentioned above, $\Pi^+(p)$ is analytic in Δ near the origin $\Delta = 0$ and can therefore be omitted in the calculation of the spectral density. All derivatives of $\Pi^+(p) \equiv \Pi^+(M - \Delta)$ with respect to Δ are represented as vacuum bubbles with one additional line carrying rising indices. Such diagrams can be efficiently calculated within the recurrence relation technique developed in Ref. [7].

Therefore one is left with the second part $\Pi^-(p)$ containing the non-analytical contributions in Δ which leads to a non-vanishing spectral density. Still the integral in Eq. (14) cannot be done analytically. In order to obtain an expansion for the spectral density near the threshold in an analytical form we make use of the asymptotic series expansion for

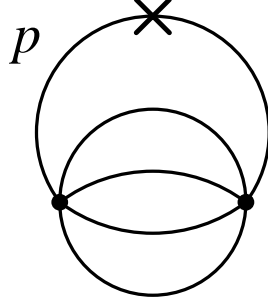


Figure 1: Representation of $\Pi^+(p)$ as vacuum bubble with added line. The cross denotes an arbitrary number of derivatives to the specified line.

the function $\Pi(x)$ which crucially simplifies the integrands but still preserves the singular structure of the integral in terms of the variable Δ . The asymptotic series expansion to order N of the main part of each propagator, i.e. of the McDonald function, is given by [33]

$$K_{\lambda,N}^{as}(z) = \left(\frac{\pi}{2z}\right)^{1/2} e^{-z} \left[\sum_{n=0}^{N-1} \frac{(\lambda, n)}{(2z)^n} + \theta \frac{(\lambda, N)}{(2z)^N} \right], \quad (\lambda, n) := \frac{\Gamma(\lambda + n - 1/2)}{n! \Gamma(\lambda - n - 1/2)} \quad (22)$$

($\theta \in [0, 1]$). Therefore the asymptotic expansion of the function $\Pi(x)$ consists of an exponential factor e^{-Mx} and an inverse power series in x up to an order \tilde{N} which is closely related to N . It is this asymptotic expansion that determines the singularity structure of the integral. We write the whole integral in the form of the sum of two terms,

$$\begin{aligned} \Pi^-(p) = & \pi^{\lambda+1} \int \left(\frac{ipx}{2}\right)^{-\lambda} H_{\lambda}^-(ipx) (\Pi(x) - \Pi_N^{as}(x)) x^{2\lambda+1+2\varepsilon} dx \\ & + \pi^{\lambda+1} \int \left(\frac{ipx}{2}\right)^{-\lambda} H_{\lambda}^-(ipx) \Pi_N^{as}(x) x^{2\lambda+1+2\varepsilon} dx = \Pi^{di}(p) + \Pi^{as}(p). \end{aligned} \quad (23)$$

The integrand of the first term $\Pi^{di}(p)$ behaves as $1/x^{\tilde{N}}$ at large x while the integrand of the second term accumulates all lower powers of the large x expansion. Note that only the large x behaviour is essential for the near threshold expansion of the spectral density. This fact has been taken into account in Eqs. (16) and (19) where we introduced a cutoff Λ . However, from the practical point of view the calculation of the regularized integrals with an explicit cutoff is inconvenient. The final result of the calculation – the spectral density

of the diagram – is independent of the cutoff, but the integration is technically complicated if the cutoff is introduced. However, in extending the integration over the whole region of the variable x without using the cutoff one immediately encounters divergences at small x because the asymptotic expansion is invalid in the region near the origin, so one is not allowed to continue the integration to this region. The standard way to cope with such a situation is to introduce dimensional regularization. It allows one to deal with divergent expressions at intermediate stages of the calculation and is technically simple because it does not introduce any cutoff and therefore does not modify the integration region drastically. Note that dimensional regularization does not necessarily regularize all divergences in this case (in contrast to the standard case of ultraviolet divergences) but nevertheless suffices for our purposes. We use a parameter ε to regularize the divergences at small x . This regularization prescription is an unorthodox version of the dimensional regularization (see e.g. Refs. [39]).

The first part $\Pi^{di}(p)$ in Eq. (23) containing a difference of the polarization function and its asymptotic expansion as the integrand gives no contributions to the spectral density up to a given order of the expansion in Δ . This is because the subtracted asymptotic series to order N cancels the inverse power behaviour of the integrand to this degree N . The integrand decreases sufficiently fast for large values of x and the integral converges even at $\Delta = 0$. Therefore this term is inessential when the expansion of the spectral density is evaluated up to some order. One can readily determine the order of the expansion near $\Delta = 0$ at which a contribution to the spectral density appears in using some further simplifications of the integrand of the term $\Pi^{di}(p)$ in Eq. (23). Namely, we replace the Hankel function under the integration sign by its asymptotic series expansion. The resulting exponential factor $e^{(p-M)t}$ can then be expanded in the parameter $\Delta = M - p$ and integrated together with the finite inverse power series in x . One obtains a finite power series in this parameter Δ which leads to a non-regular term of order Δ^N (for instance, $\Delta^N \ln \Delta$ or $\Delta^N \sqrt{\Delta}$). Therefore the part $\Pi^{di}(p)$ is regular and gives no contribution to

the spectral density up to the order Δ^N . For this reason we concentrate on the expansion of the second part $\Pi^{as}(p)$ and find that only this part contains the contribution to the spectral density up to the N .

Therefore the expansion of the spectral density at small E is determined only by the integral $\Pi^{as}(p)$ of Eq. (23). This integral is still rather complicated to compute but we can go a step further in its analytical evaluation. Indeed, since the singular behaviour of $\Pi^{as}(p)$ is determined by the behaviour at large x , we can replace the first factor, i.e. the Hankel function, in the large x region by its asymptotic expansion up to some order N . We use

$$H_{\lambda,N}^{-as}(iz) = \left(\frac{2}{\pi z}\right)^{1/2} e^{z+i\lambda\pi/2} \left[\sum_{n=0}^{N-1} \frac{(-1)^n(\lambda, n)}{(2z)^n} + \theta \frac{(-1)^N(\lambda, N)}{(2z)^N} \right] \quad (24)$$

(cf. Eq. (22) for the notation) to obtain a representation

$$\Pi^{das}(p) = \pi^{\lambda+1} \int \left(\frac{ipx}{2}\right)^{-\lambda} H_{\lambda,N}^{-as}(ipx) \Pi_N^{as}(x) x^{2\lambda+1+2\varepsilon} dx. \quad (25)$$

The index “*das*” stands for “double asymptotic” and indicates that the integrand in Eq. (25) consists of a product of two asymptotic expansions: one for the polarization function $\Pi(x)$ and another for the Hankel function $H_{\lambda}^{-}(x)$ as weight (or kernel). Both asymptotic expansions are straightforward and can be obtained from standard handbooks on Bessel functions. We therefore arrive at our final result: the integration necessary for evaluating the near threshold expansion of the water melon diagrams reduces to integrals of the type of Euler’s Gamma function, i.e. integrals containing exponentials and powers. Indeed, the result of the expansion in Eq. (25) is an exponential function $e^{-\Delta x}$ times a power series in $1/x$, namely

$$x^{-a+2\varepsilon} e^{-\Delta x} \sum_{j=0}^{N-1} \frac{A_j}{x^j} \quad (26)$$

where a has already been defined in Eq. (17) and the coefficients A_j are simple functions of the momentum p and the masses m_i . The expression in Eq. (26) can be integrated analytically using

$$\int_0^\infty x^{-a+2\varepsilon} e^{-\Delta x} dx = \Gamma(1-a+2\varepsilon) \Delta^{a-1-2\varepsilon}. \quad (27)$$

The result is

$$\Pi^{das}(M - \Delta) = \sum_{j=0}^{N-1} A_j \Gamma(1 - a - j + 2\varepsilon) \Delta^{a+j-1-2\varepsilon}. \quad (28)$$

This expression is our final representation for the part of the polarization function of a water melon diagram necessary for the calculation of the spectral density near the production threshold. It is also one of the main results of our paper.

Next we discuss the general structure of the expression in Eq. (28) in detail. In the case where a takes integer values, these coefficients result in $1/\varepsilon$ -divergences for small values of ε . The powers of Δ in Eq. (28) have to be expanded to first order in ε and give

$$\frac{1}{2\varepsilon} \Delta^{2\varepsilon} = \frac{1}{2\varepsilon} + \ln \Delta + O(\varepsilon). \quad (29)$$

Because of

$$\text{Disc } \ln(\Delta) \equiv \ln(-E - i0) - \ln(-E + i0) = -2\pi i \theta(E) \quad (30)$$

$\Pi^{das}(M - \Delta)$ in Eq. (28) contributes to the spectral density. For half-integer values of a the power of Δ itself has a cut even for $\varepsilon = 0$. The discontinuity is then given by

$$\text{Disc } \sqrt{\Delta} = -2i\sqrt{E} \theta(E). \quad (31)$$

Our method to construct a threshold expansion thus simply reduces to the analytical calculation of the integral in Eq. (25) which can be done for arbitrary dimension and an arbitrary number of lines with different masses. In the next subsections we use our technique to work out some specific examples which demonstrate both the simplicity and efficiency of our method.

3.1 Equal mass sunset diagram

The polarization function represented by the sunset diagram with three propagators with equal masses m in $D = 4$ space-time dimensions is given by

$$\Pi(x) = \frac{m^3 K_1(mx)^3}{(2\pi)^6 x^3}. \quad (32)$$

The exact spectral density is given by the integral representation in Eq. (8) which for this particular case reads

$$\rho(s) = \frac{2\pi}{i\sqrt{s}} \int_{c-i\infty}^{c+i\infty} I_1(\zeta\sqrt{s})\Pi(\zeta)\zeta^2 d\zeta. \quad (33)$$

In order to obtain a threshold expansion of the spectral density in Eq. (33) we use Eq. (28) to calculate the expansion of the appropriate part of the polarization function. To illustrate the procedure we present the explicit shape of the integrand in Eq. (25) which is given by an asymptotic expansion at large x ,

$$\begin{aligned} \pi^2 \left(\frac{ipx}{2}\right)^{-1} H_{1,N}^{as}(px) \Pi_N^{as}(x) x^{3+2\varepsilon} &= \frac{m^{3/2} e^{(p-3m)x}}{(4\pi)^3 p^{3/2}} x^{-3+2\varepsilon} \times \\ &\times \left\{ 1 + \frac{9}{8mx} - \frac{3}{8px} + \frac{9}{128m^2x^2} - \frac{27}{64mpx^2} - \frac{15}{128p^2x^2} + O(x^{-3}) \right\}. \end{aligned} \quad (34)$$

From Eq. (34) we can easily read off the coefficients A_j that enter the expansion in Eq. (26). The spectral density is obtained by performing the term-by-term integration of the series in Eq. (34) and by evaluating the discontinuity across the cut along the positive energy axis $E > 0$. The result reads

$$\begin{aligned} \tilde{\rho}(E) &= \frac{E^2}{384\pi^3\sqrt{3}} \left\{ 1 - \frac{1}{2}\eta + \frac{7}{16}\eta^2 - \frac{3}{8}\eta^3 + \frac{39}{128}\eta^4 - \frac{57}{256}\eta^5 \right. \\ &\quad \left. + \frac{129}{1024}\eta^6 - \frac{3}{256}\eta^7 - \frac{4047}{32768}\eta^8 + \frac{18603}{65536}\eta^9 - \frac{248829}{524288}\eta^{10} + O(\eta^{11}) \right\} \end{aligned} \quad (35)$$

where the notation $\eta = E/M$, $M = 3m$ is used. The simplicity of the derivation is striking. By no cost it can be generalized to any number of lines, arbitrary masses, and any space-time dimension. The standard equal mass sunset is chosen for the definiteness only. It also allows us to compare our results with results available in the literature. Eq. (35) reproduces the expansion coefficients \tilde{a}_j obtained in Ref. [31] (the fourth column in Table 1 of Ref. [31]) by a direct integration in momentum space within the technique of region separation [40].

The case of the equal mass standard sunset diagram is the simplest one. There exists an analytical expression for the spectral density of the sunset diagram with three equal

mass propagators in $D = 4$ space-time dimensions in terms of elliptic integrals [41] (see also Ref [42]¹). This expression can be used for a comparison with our exact result in Eq. (33) or with the expansion in Eq. (35). However, we only present the result for $D = 2$ in order to keep the resulting expressions in a reasonably short form (cf. Ref. [43]). In $D = 2$ space-time dimensions the spectral density for a sunset diagram with equal masses m can be readily obtained. We just use the exact expression for the spectral density in the convolution representation [7] and proceed towards $n = 3$ equal masses. The convolution function for two spectral densities in $D = 2$ dimensional space-time ($\lambda = 0$) reads

$$\rho(s; s_1; s_2) = \frac{1}{2\pi\sqrt{(s - s_1 - s_2)^2 - 4s_1s_2}}. \quad (36)$$

The two spectral densities one has to convolute are the spectral density of a correlator with two equal masses and the spectral density of a single massive line. While the latter is given by $\rho(s; m^2) = \delta(s - m^2)$, the former can be obtained from Eq. (36) by inserting $s_1 = s_2 = m^2$,

$$\rho(s; m^2; m^2) = \frac{1}{2\pi\sqrt{s(s - 4m^2)}}. \quad (37)$$

So the convolution leads to

$$\begin{aligned} \rho(s; m^2; m^2; m^2) &= \frac{1}{4\pi^2} \int_{4m^2}^{(\sqrt{s}-m)^2} \frac{dt}{\sqrt{(s - m^2 - t)^2 - 4m^2t}\sqrt{t(t - 4m^2)}} \\ &= \frac{1}{4\pi^2} \int_{4m^2}^{(\sqrt{s}-m)^2} \frac{dt}{\sqrt{t(t - 4m^2)((\sqrt{s} + m)^2 - t)((\sqrt{s} - m)^2 - t)}}. \end{aligned} \quad (38)$$

Now we use the relation (cf. Ref. [41])

$$\int_{t_1}^{t_2} \frac{dt}{\sqrt{(t - t_0)(t - t_1)(t_2 - t)(t_3 - t)}} = \frac{2}{\sqrt{(t_3 - t_1)(t_2 - t_0)}} K(k^2), \quad (39)$$

$$k^2 = \frac{(t_2 - t_1)(t_3 - t_0)}{(t_3 - t_1)(t_2 - t_0)} \quad (40)$$

¹We thank A. Davydychev for bringing these papers to our attention.

with $t_3 > t_2 > t > t_1 > t_0$ and the definition of the complete elliptic integral of the first kind

$$K(k^2) = \int_0^{\pi/2} \frac{d\varphi}{\sqrt{1 - k^2 \sin^2 \varphi}} = F\left(\frac{\pi}{2}, k^2\right) \quad (41)$$

(remark the difference in the definition) for $t_0 = 0$, $t_1 = 4m^2$, $t_2 = (\sqrt{s} - m)^2$, and $t_3 = (\sqrt{s} + m)^2$ to perform the integration in Eq. (38). We obtain

$$k^2 = \frac{((\sqrt{s} - m)^2 - 4m^2)(\sqrt{s} + m)^2}{((\sqrt{s} + m)^2 - 4m^2)(\sqrt{s} - m)^2} \quad (42)$$

and finally end up with

$$\rho(s; m^2; m^2; m^2) = \frac{K(k^2)}{2\pi^2(\sqrt{s} - m)\sqrt{(\sqrt{s} + m)^2 - 4m^2}}. \quad (43)$$

Therefore the spectral density in terms of the energy E reads (see e.g. Ref. [44])

$$\begin{aligned} \tilde{\rho}(E) &= \frac{1}{2\pi^2(2m + E)\sqrt{(4m + E)^2 - 4m^2}} K(k^2), \\ k^2 &= \frac{((2m + E)^2 - 4m^2)(4m + E)^2}{((4m + E)^2 - 4m^2)(2m + E)^2}, \quad M = 3m. \end{aligned} \quad (44)$$

By expanding the elliptic integral in terms of the threshold parameter E one reproduces the threshold expansion in Eq. (35). The result for $D = 4$ space-time dimensions is expressible by the elliptic integrals with some rational functions as factors that makes the result a bit longer. Note that the representation in Eq. (44) is understood to be an analytical expression for the spectral density. However, it is a matter of taste whether the representation through the elliptic integrals as in Eq. (44) is considered simpler (or in a more analytical form) than the integral representation in Eq. (8). The only objection against the latter which one can find in the literature is that the Bessel functions are complicated (see e.g. Ref. [30]). But after more than a century of intensive investigation they are well-known and no more complicated than the square root of the fourth order polynomial which is used in Eq. (39) to define the elliptic integral.

3.2 Equal mass water melon diagrams with four or more propagators

The water melon diagrams with four or more propagators cannot be easily done by using the momentum space technique because it requires the multiloop integration of entangled momenta. Within the configuration space technique the generalization to any number of lines (or loops) is immediate by no effort. Consider first a three-loop case of water melon diagrams (also called banana diagrams [28] or basketball diagrams [13]). The polarization function of the equal mass water melon diagram with four propagators in $D = 4$ space-time is given by

$$\Pi(x) = \frac{m^4 K_1(mx)^4}{(2\pi)^8 x^4}. \quad (45)$$

The exact spectral density of this diagram can be obtained from Eq. (33) while the near threshold expansion can be found using Eq. (28). We construct the expansion of the spectral density near threshold explicitly and compare it with the exact result. The expansion of the integrand (cf. Eq. (25)) reads

$$\begin{aligned} \pi^2 \left(\frac{ipx}{2} \right)^{-1} H_{1,N}^{as}(px) \Pi_N^{as}(x) x^{3+2\varepsilon} &= \frac{m^2 e^{(p-4m)x}}{(4\pi)^4 \sqrt{2\pi} p^{3/2}} x^{-9/2+2\varepsilon} \times \\ &\times \left\{ 1 + \frac{3}{2mx} - \frac{3}{8px} + \frac{3}{8m^2 x^2} - \frac{15}{128p^2 x^2} - \frac{9}{16mpx^2} + O(x^{-3}) \right\}. \end{aligned} \quad (46)$$

After the integration and the calculation of the discontinuity we obtain the expansion of the spectral density in the form

$$\begin{aligned} \tilde{\rho}(E) &= \frac{E^{7/2} M^{1/2}}{26880\pi^5 \sqrt{2}} \left\{ 1 - \frac{1}{4}\eta + \frac{81}{352}\eta^2 - \frac{2811}{18304}\eta^3 + \frac{17581}{292864}\eta^4 \right. \\ &\quad \left. + \frac{1085791}{19914752}\eta^5 - \frac{597243189}{3027042304}\eta^6 + \frac{4581732455}{12108169216}\eta^7 - \frac{496039631453}{810146594816}\eta^8 + O(\eta^9) \right\} \end{aligned} \quad (47)$$

where $\eta = E/M$ and $M = 4m$ is the threshold value. One sees the difference with the previous three-line case. In Eq. (47) the cut represents the square root branch while in the three-line case it was a logarithmic cut. One can easily figure out the reason for this by looking at the asymptotic structure of the integrand. For even number of lines (i.e.

odd number of loops) it is a square root branch, while for an odd number of lines (even number of loops) it is a logarithmic branch. This is true in even space-time dimensions. In the general case the structure of the cut depends on the dimensionality of the space-time as well. The general formula reads

$$\tilde{\rho}(E) \sim E^{(\lambda+1/2)(n-1)-1}(1 + O(E)). \quad (48)$$

For $D = 4$ space-time dimension (i.e. $\lambda = 1$) we can verify the result of Ref. [7] (cf. Eq. (48)),

$$\tilde{\rho}(E) \sim E^{(3n-5)/2}(1 + O(E)). \quad (49)$$

Numerically Eq. (47) reads

$$\begin{aligned} \tilde{\rho}(E) = & 8.5962 \cdot 10^{-5} E^{7/2} M^{1/2} \{ 1.000 - 0.250\eta + 0.230\eta^2 \\ & - 0.154\eta^3 + 0.060\eta^4 + 0.055\eta^5 - 0.197\eta^6 + 0.378\eta^7 - 0.612\eta^8 + O(\eta^9) \} \end{aligned} \quad (50)$$

where we have written down the coefficients up to three decimal places. It is difficult to say anything definite about the convergence of this series. By construction it is an asymptotic series. However, we stress that the practical (or explicit) convergence can always be checked by comparing series expansions like the one shown in Eq. (50) with the exact spectral density given in Eq. (33) by numerical integration.

We conclude this part of the paper by the statement that the spectral density of the water melon diagram is most efficiently calculable within the configuration space technique. Whether it is the exact result or the expansion, the configuration space technique can readily deliver the desired result. The exact formula in Eq. (33) as well as the threshold expansion obtained from it can be used to calculate the spectral density for an arbitrarily large number of internal lines. We stress that the case of different masses does not lead to any complications within the configuration space technique: the exact formula in Eq. (8) and/or the near threshold expansion work equally well for any arrangement of masses. We do not present plots for general cases of different masses because they are not very

illustrative, showing only the common threshold. However, there is some interesting kinematic regime for different masses which is important for applications and which, to our best knowledge, have not been touched earlier. An analytical solution for the expansion of the spectral density in this regime is given in the next section.

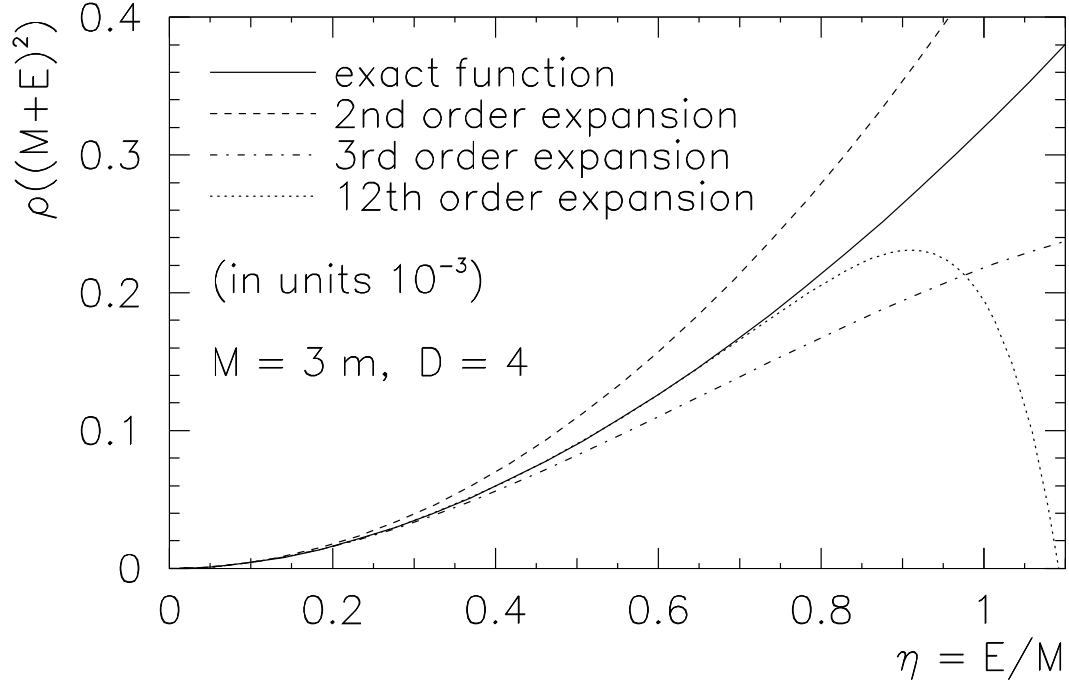


Figure 2: Various results for the spectral density for $n = 3$ equal masses in $D = 4$ space-time dimensions in dependence on the threshold parameter E/M . Shown are the exact solution obtained by using Eq. (33) (solid curve) and threshold expansions for different orders taken from Eq. (35) (dashed to dotted curves).

4 Strongly asymmetric case $m_0 \ll M$

The threshold expansion for equal (or close) masses breaks down for $E \approx M = \sum m_i$. The example is shown in Fig. 2 for the $D = 4$ proper sunset. However, if the masses are not equal, the region of the break-down of the expansion is determined by the mass with the smallest numerical value. The simplest example where one can see this phenomenon

is the analytical expression for the spectral density of the simple loop (degenerate water melon diagram) with two different masses m_1 and m_2 . In $D = 4$ space-time dimensions (see e.g. Ref. [7]) one has

$$\tilde{\rho}(E) = \frac{\sqrt{E(E + 2m_1)(E + 2m_2)(E + 2M)}}{(4\pi(M + E))^2} \quad (51)$$

where $M = m_1 + m_2$. The threshold expansion is obtained by expanding the right hand side of Eq. (51) in E for small values of E . If m_2 is much smaller than m_1 , the expansion breaks down at $E \approx 2m_2$. The break-down of the series expansion can also be observed in more general cases. If one of the masses (which we call m_0) is much smaller than the other masses, the threshold expansion is only valid in a very limited region $E \lesssim 2m_0$.

To generalize the expansion and extend it to the region of $E \sim M$ one has to treat the smallest mass exactly. In this case one can use a method which we call the resummation of the smallest mass contributions. Below we describe the resummation technique. We start with the representation

$$\Pi^{pas}(p) = \pi^{\lambda+1} \int \left(\frac{ipx}{2} \right)^{-\lambda} H_{\lambda,N}^{-as}(ipx) \Pi_{m_0}^{as}(x) x^{2\lambda+1+2\varepsilon} dx \quad (52)$$

which is the part of the polarization function contributing to the spectral density. The integrand in Eq. (52) has the form

$$\Pi_{m_0}^{as}(x) = \Pi_{n-1}^{as}(x) D(m_0, x) \quad (53)$$

where the asymptotic expansions are substituted for all the propagators except for the one with the small mass m_0 . This is indicated by the index “*pas*” in Eq. (52) which stands for “partial asymptotic”. The main technical observation leading to the generalization of the expansion method is that $\Pi^{pas}(p)$ is still analytically computable in a closed form. Indeed, the genuine integral to compute has the form

$$\begin{aligned} \int_0^\infty x^{\mu-1} e^{-\tilde{\alpha}x} K_\nu(\beta x) dx &= \\ &= \frac{\sqrt{\pi}(2\beta)^\nu}{(2\tilde{\alpha})^{\mu+\nu}} \frac{\Gamma(\mu+\nu)\Gamma(\mu-\nu)}{\Gamma(\mu+1/2)} {}_2F_1\left(\frac{\mu+\nu}{2}, \frac{\mu+\nu+1}{2}; \mu+\frac{1}{2}; 1 - \frac{\beta^2}{\tilde{\alpha}^2}\right) \end{aligned} \quad (54)$$

where $\tilde{\alpha} = \Delta - m_0$ and $\beta = m_0$. The integral $\Pi^{pas}(p)$ in Eq. (52) is thus expressible in terms of hypergeometric functions [45, 46]. For constructing the spectral density, being our main concern as mentioned before, one has to find the discontinuity of the right hand side of Eq. (54). There are several ways to do this. We proceed by applying the discontinuity operation to the integrand of the integral representation of the hypergeometric function. The resulting integrals are calculated again in terms of hypergeometric functions. Indeed,

$$\begin{aligned} \frac{1}{2\pi i} \text{Disc} \int_0^\infty x^{\mu-1} e^{\alpha x} K_\nu(\beta x) dx &= \\ &= \frac{2^\mu (\alpha^2 - \beta^2)^{1/2-\mu}}{\alpha^{1/2-\nu} \beta^\nu} \frac{\Gamma(3/2)}{\Gamma(3/2 - \mu)} {}_2F_1 \left(\frac{1-\mu-\nu}{2}, \frac{2-\mu-\nu}{2}; \frac{3}{2} - \mu; 1 - \frac{\beta^2}{\alpha^2} \right) \end{aligned} \quad (55)$$

where $\alpha = E + m_0$. The final expression in Eq. (55) completely solves the problem of the generalization of the near threshold expansion technique. For integer values of μ there are no singular Gamma functions (with negative integer argument). Therefore we can lift up the regularization and set $\varepsilon = 0$ when using this expression. We thus have found a direct transition from the polarization function as expressed through the integral to the spectral density in terms of one hypergeometric function for each genuine integral. There is no need to use the recurrence relations available for hypergeometric functions.

In the following subsections we give explicit examples for $D = 4$ and compare with the exact result in Eq. (33) and the pure expansion near the threshold. In the following the standard threshold expansion without resummation is called the pure threshold expansion.

4.1 The two-line water melon with a small mass

We start with a (over)simplified example of the two-line diagram with masses m and $m_0 \ll m$ in four space-time dimensions. In this example the expansion of the spectral density and its generalized expansion can be readily compared analytically with the exact result in Eq. (51). This is the feature that justifies our discussion in this section. The results for the spectral density of this diagram are shown in Fig. 3. The solid curve displays the exact result obtained by using Eq. (33) (which reproduces the analytical expression

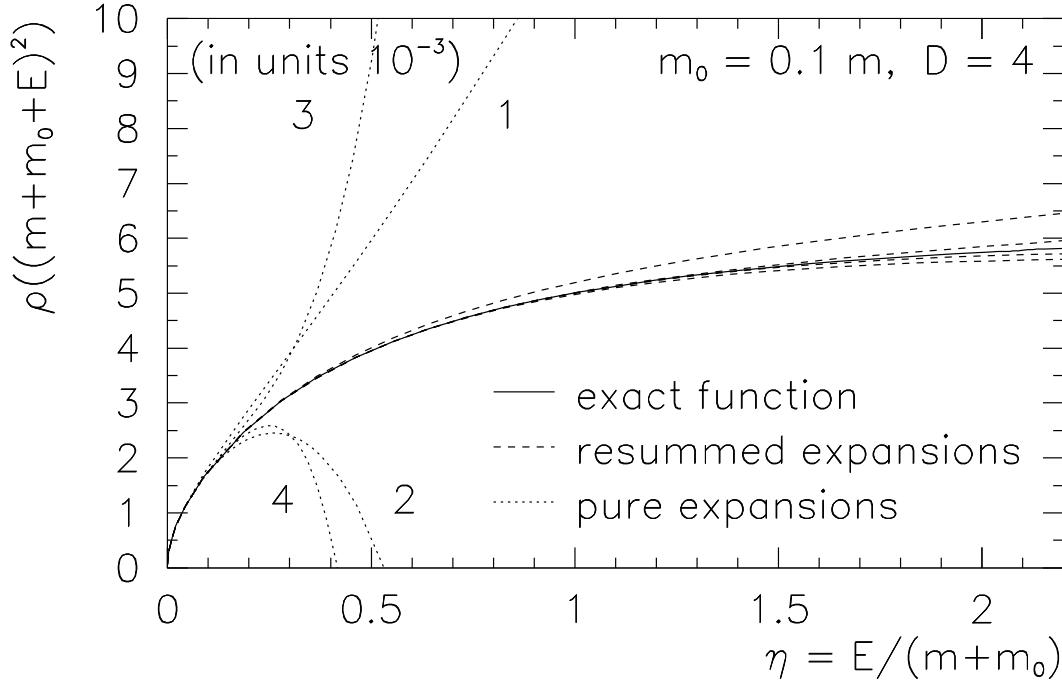


Figure 3: Various solutions for the spectral density for two masses m and $m_0 \ll m$ and $D = 4$ space-time dimensions. Shown are the exact solution which is obtained by using Eq. (33) (solid curve), the pure threshold expansions using Eq. (56) (dotted curves), and the solutions for the resummation of the smallest mass contributions like in Eq. (57) (dashed curves), both expansions from the first up to the fourth order in the asymptotic expansion. For the pure threshold expansion the order is indicated explicitly.

in Eq. (51)). We compare this result with the two expansions.

The pure expansion of the spectral density near threshold (the second order asymptotic expansion should suffice to show the general features in a short and concise form) is given by

$$\begin{aligned} \tilde{\rho}^{das}(E) = & \frac{\sqrt{2m_0mE}}{8\pi^2M^{3/2}} \left\{ 1 + \left(\frac{1}{m} + \frac{1}{m_0} - \frac{7}{M} \right) \frac{E}{4} \right. \\ & \left. - \left(\frac{1}{m_0^2} + \frac{1}{m^2} + \frac{12}{m_0m} - \frac{79}{M^2} \right) \frac{E^2}{32} + O(E^3) \right\} \end{aligned} \quad (56)$$

where $M = m + m_0$. As mentioned above, this series breaks down for $E > 2m_0$ (see Eq. (51)). If we look at the dotted curves in Fig. 3 this becomes obvious. Here we have

plotted the series expansions up to the fourth order with the mass arrangement $m_0 = m/10$. The dashed lines represent the resummation of the smallest mass contributions. The analytical expression for the spectral density of the polarization function in Eq. (52) for the generalized asymptotic expansion based on Eq. (55) is given by

$$\begin{aligned} \tilde{\rho}^{pas}(E) = & \frac{\sqrt{mE(E+2m_0)}}{8\pi^2(E+M)^{3/2}} \left\{ {}_2F_1\left(0, \frac{1}{2}; \frac{3}{2}; 1 - \frac{m_0^2}{(E+m_0)^2}\right) \right. \\ & + \frac{E(E+2m_0)}{8m(E+M)} {}_2F_1\left(\frac{1}{2}, 1; \frac{5}{2}; 1 - \frac{m_0^2}{(E+m_0)^2}\right) \\ & \left. - \frac{E^2(E+2m_0)^2}{128m^2(E+M)^2} \left(1 + \frac{16m(E+M)}{5(E+m_0)^2}\right) {}_2F_1\left(1, \frac{3}{2}; \frac{7}{2}; 1 - \frac{m_0^2}{(E+m_0)^2}\right) + \dots \right\}. \end{aligned} \quad (57)$$

We have set the regularization parameter $\varepsilon = 0$ because the spectral density is finite. With $\varepsilon = 0$ the resulting expressions for the hypergeometric functions in Eq. (55) simplify. The first term in the curly brackets of Eq. (57) is obviously equal to 1 in this limit because the first parameter of the hypergeometric function vanishes for $\varepsilon = 0$. However, we keep Eq. (57) in its given form to show the structure of the contributions. The generalized threshold expansion has the form

$$\tilde{\rho}^{pas}(E) = g_0(E, m_0) + E g_1(E, m_0) + E^2 g_2(E, m_0) + \dots \quad (58)$$

where the functions $g_j(E, m_0)$ represent effects of the resummation of the smallest mass and are not polynomials in the threshold parameter E . In the simple two-line case the hypergeometric functions reduce to elementary functions. For instance,

$$\begin{aligned} {}_2F_1\left(\frac{1}{2}, 1; \frac{5}{2}; 1 - \frac{m_0^2}{(E+m_0)^2}\right) = & \\ = & \frac{3(E+m_0)}{2E(E+2m_0)} \left(E + m_0 - \frac{m_0^2}{2\sqrt{E(E+2m_0)}} \ln \left(\frac{E+m_0 + \sqrt{E(E+2m_0)}}{E+m_0 - \sqrt{E(E+2m_0)}} \right) \right). \end{aligned} \quad (59)$$

Higher order contributions are given by hypergeometric functions with larger numerical values of the parameters. They can be simplified by using Gaussian recurrence relations for hypergeometric functions (see e.g. Ref. [45]).

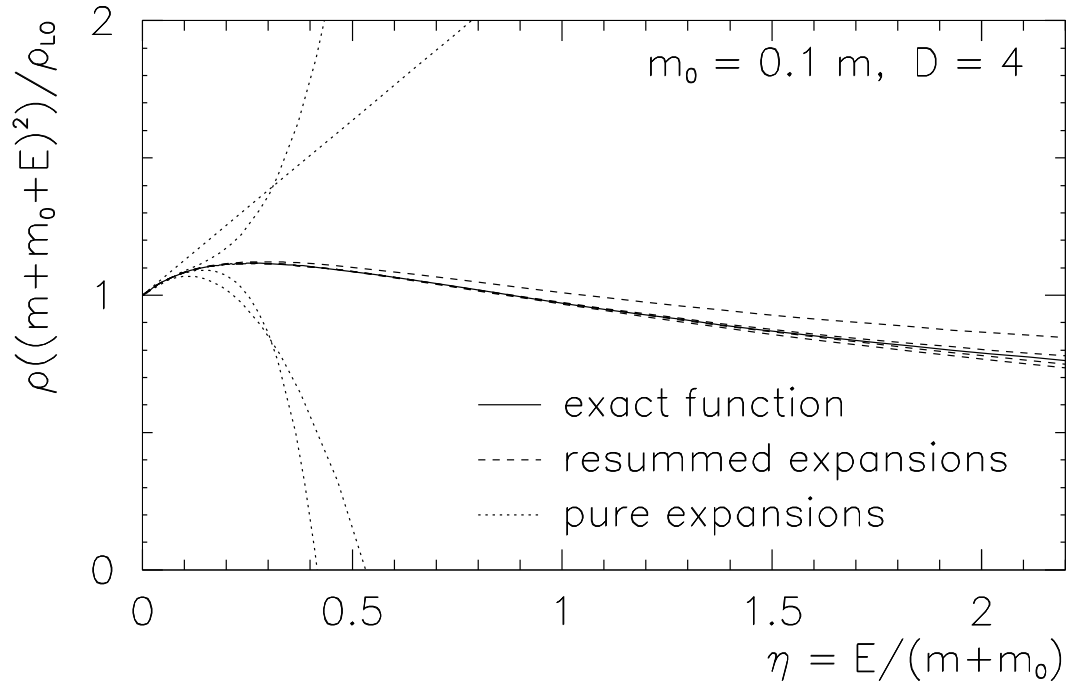


Figure 4: The same as Fig. 3 where the spectral density is normalized to the leading order expression of the pure threshold expansion.

The convergence of the expansion in Eq. (57) breaks down only at $E \sim M = m + m_0$. The resummation leads to an essential improvement of the convergence in comparison with the pure threshold expansion. In Fig. 4 we show the same curves divided by the leading order term. This representation is more convenient for the diagrams which we will discuss in following subsections.

Note that Eq. (59) does not lead to the exact function in Eq. (51) because terms of order E^N stemming from the difference part $\Pi^{di}(p)$ of the correlator are missing. It simply corrects the behaviour of the coefficient functions by the small mass contributions.

4.2 The sunset diagram with a small mass

Here we analyze the sunset diagram with two equal masses m and a third mass $m_0 \ll m$ ($m_0 = m/10$). The exact result obtained by using Eq. (33) and normalized to the leading

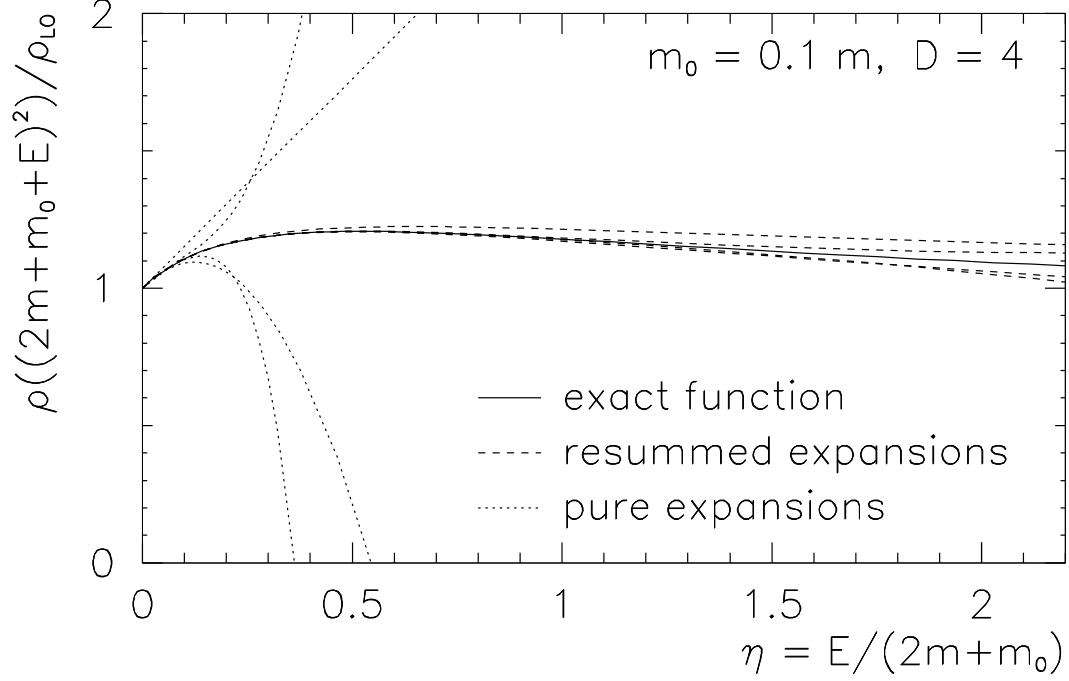


Figure 5: The spectral density for the sunset diagram in $D = 4$ space-time dimensions with a tiny mass m_0 , normalized to the general power behaviour. Shown are the exact result obtained by using Eq. (33) (solid curve), the threshold expansion according to Eq. (60) (dotted curves), and the result for the resummation of the smallest mass contributions according to Eq. (61) (dashed curves).

order term is shown in Fig. 5 as the solid curve. The pure expansion near the threshold reads

$$\begin{aligned}
 \tilde{\rho}^{das}(E) = & \frac{mE^2\sqrt{m_0M}}{128\pi^3M^2} \left\{ 1 + \left(\frac{1}{m_0} + \frac{2}{m} - \frac{13}{M} \right) \frac{E}{8} \right. \\
 & \left. - \left(\frac{5}{m_0^2} + \frac{4}{m^2} + \frac{39}{m_0m} + \frac{153}{mM} - \frac{1115}{M^2} \right) \frac{E^2}{512} + O(E^3) \right\}. \quad (60)
 \end{aligned}$$

It is shown by the dotted curves in Fig. 5. In case of the resummation of the smallest mass contributions we obtain hypergeometric functions which do not obviously reduce to elementary functions in this case. The result for the spectral density within the asymptotic

expansion up to the second order in Eq. (52) is given by

$$\begin{aligned} \tilde{\rho}^{pas}(E) = & \frac{mE^2(E+2m_0)^2}{512\pi^3(E+m_0)^{3/2}(E+M)^{3/2}} \left\{ {}_2F_1\left(\frac{3}{4}, \frac{5}{4}; 3; 1 - \frac{m_0^2}{(E+m_0)^2}\right) \right. \\ & + \frac{E(E+2m_0)}{8m(E+M)} \left(1 + \frac{3m}{2(E+m_0)}\right) {}_2F_1\left(\frac{5}{4}, \frac{7}{4}; 4; 1 - \frac{m_0^2}{(E+m_0)^2}\right) \\ & - \frac{E^2(E+2m_0)^2}{512m^2(E+M)^2} \left(1 + \frac{5m}{2(E+m_0)}\right) \left(1 + \frac{9m}{2(E+m_0)}\right) \times \\ & \left. {}_2F_1\left(\frac{7}{4}, \frac{9}{4}; 5; 1 - \frac{m_0^2}{(E+m_0)^2}\right) \right\}. \end{aligned} \quad (61)$$

We see that the dashed curves in Fig. 5 that represent the result in Eq. (61) approximate the exact curve much better than the dotted curves.

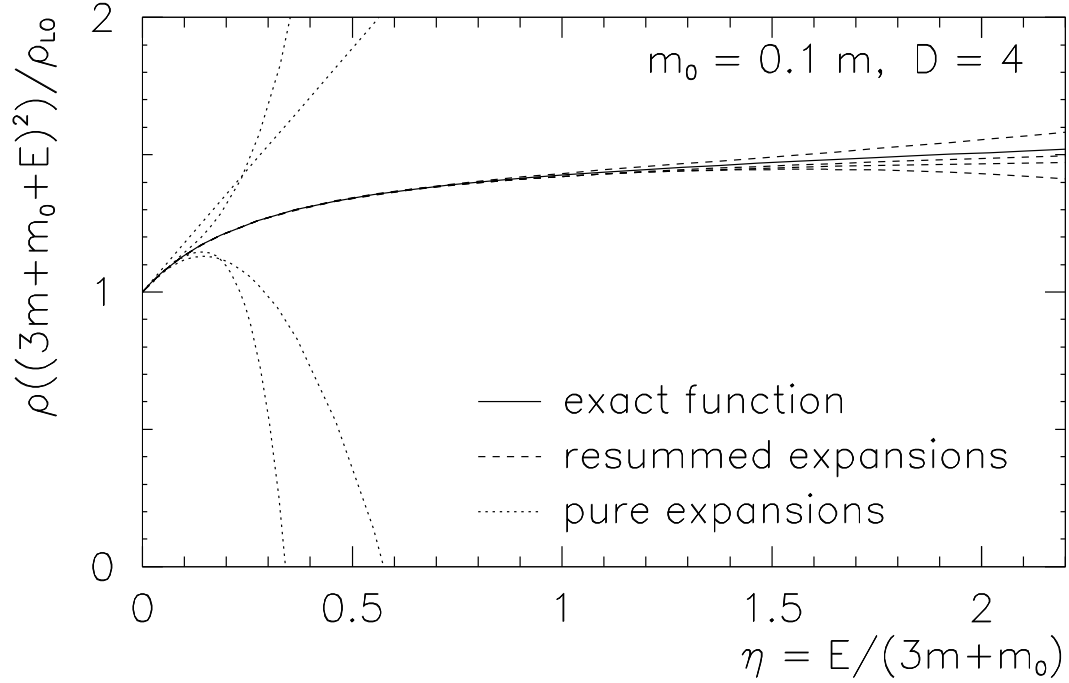


Figure 6: The spectral density for the four-line water melon diagram in $D = 4$ space-time dimensions with a tiny mass m_0 , normalized to the general power behaviour. Shown are the exact result obtained by using Eq. (33) (solid curve), the threshold expansion according to Eq. (62) (dotted curves), and the result for the resummation of the smallest mass contributions according to Eq. (63) (dashed curves).

4.3 The four-line water melon with a small mass

With this example we conclude our consideration of the strongly asymmetric case and at the same time show the way to the multi-line water melon diagrams which can be treated in an analogous manner. The result for the exact expression obtained by using Eq. (33) is shown in Fig. 6 as a solid line, normalized to the leading order term. The dotted lines represent the results for the pure expansion near threshold which is given by

$$\begin{aligned} \tilde{\rho}^{das}(E) = & \frac{m^{3/2} E^{7/2} \sqrt{2m_0}}{3360\pi^5 M^{3/2}} \left\{ 1 + \left(\frac{1}{m_0} + \frac{3}{m} - \frac{19}{M} \right) \frac{E}{12} \right. \\ & \left. - \left(\frac{5}{m_0^2} - \frac{3}{m^2} + \frac{28}{m_0 m} + \frac{368}{mM} - \frac{2195}{M^2} \right) \frac{E^2}{1056} + O(E^3) \right\}. \end{aligned} \quad (62)$$

The asymptotic expansion to the second order in Eq. (52) gives

$$\begin{aligned} \tilde{\rho}^{pas}(E) = & \frac{m^{3/2} E^{7/2} (E + 2m_0)^{7/2}}{26880\pi^5 (E + m_0)^3 (E + M)^{3/2}} \left\{ {}_2F_1 \left(\frac{3}{2}, 2; \frac{9}{2}; 1 - \frac{m_0^2}{(E + m_0)^2} \right) \right. \\ & + \frac{E(E + 2m_0)}{8m(E + M)} \left(1 + \frac{8m}{3(E + m_0)} \right) {}_2F_1 \left(2, \frac{5}{2}; \frac{11}{2}; 1 - \frac{m_0^2}{(E + m_0)^2} \right) \\ & \left. + \frac{E^2(E + 2m_0)^2}{1408(E + M)^2} \left(1 - \frac{32m^2}{3(E + m_0)^2} \right) {}_2F_1 \left(\frac{5}{2}, 3; \frac{13}{2}; 1 - \frac{m_0^2}{(E + m_0)^2} \right) \right\}. \end{aligned} \quad (63)$$

In Fig. 6 one can see how the expansion improves if the resummation of the smallest mass contributions (displayed as dashed lines) is performed.

The result of this section is quite general and applicable to all cases of one small mass. For some particular arrangement of masses one can obtain even simpler expressions as discussed in the next section.

4.4 The convolution with a small mass

In this section we obtain a result for the resummation of the smallest mass effects along a different route, namely, via the convolution of spectral densities. However, this method works in a narrower kinematic region than the method described in the previous section.

In $D = 4$ space-time dimensions, the convolution weight is given by

$$\rho(s; s_1; s_2) = \frac{1}{(4\pi)^2 s} \sqrt{(s - s_1 - s_2)^2 - 4s_1 s_2}. \quad (64)$$

The upper limit of the integration is determined by the requirement of positivity of the square root argument. The zeros of the square root with respect to s_2 are given by $s_2^\pm = (\sqrt{s} \pm \sqrt{s_1})^2$, and the demand $(s_2 - s_2^+)(s_2 - s_2^-) > 0$ together with $s_2^+ > s_2^-$ leads to $s_2 > s_2^+$ or $s_2 < s_2^-$. The physical region is the latter one. With $\rho_1(s) = \delta(s - m_0^2)$ for the spectral density of the single small mass line we obtain

$$\begin{aligned}\rho(s) &= \int_0^\infty ds_1 \int_{M'^2}^{(\sqrt{s}-\sqrt{s_1})^2} ds_2 \rho(s; s_1; s_2) \rho_1(s_1) \rho_2(s_2) = \\ &= \frac{1}{(4\pi)^2 s} \int_{M'^2}^{(\sqrt{s}-m_0)^2} \sqrt{(s - m_0^2 - s_2)^2 - 4m_0^2 s_2} \rho_2(s_2) ds_2\end{aligned}\quad (65)$$

where the low limit of integration is $M' = M - m_0$. We insert $s = (M + E)^2$ and $s_2 = (M' + E')^2$ and obtain

$$\begin{aligned}\tilde{\rho}(E) &= \frac{1}{(4\pi)^2 (M + E)^2} \int_0^E \sqrt{(E - E')(E + E' + 2M) + m_0^2} \times \\ &\quad \times \sqrt{(E - E' + 2m_0)(E + E' + 2M') + m_0^2} \frac{\tilde{\rho}'(E') dE'}{2(M' + E')}\end{aligned}\quad (66)$$

where $\tilde{\rho}'(E') = \rho_2((M' + E')^2)$. For this function we use the threshold expansion in E'/M' as expansion parameter. For small $E < M'$ the threshold expansion inserted for $\tilde{\rho}'(E')$ is valid because $E < M'$ implies $E' < M'$. The described procedure can be extended to the case of a very light sub-block of the diagram, e.g. a light fish diagram. In this case we have to replace $\rho_1(s)$ by the spectral density of the light sub-diagram which is well-known.

5 Recovering $\Pi(p)$ through $\rho(s)$ near threshold

The analytic structure of water melon diagrams is completely fixed by the dispersion representation. Therefore we have focussed on the computation of the spectral density as the basic quantity important both for applications and the theoretical investigation of the diagram. However, with an analytical expression for the spectral density $\rho(s)$ at hand we can readily reconstruct the non-analytic piece of the polarization function in momentum

space by using the dispersion relation

$$\Pi(p) = \int \frac{\rho(s)ds}{s - p^2}. \quad (67)$$

We rewrite this equation in terms of threshold parameters according to $p = M - \Delta$ and $s = (M + E)^2$ and obtain

$$\tilde{\Pi}(\Delta) \equiv \Pi(M - \Delta) = \int_0^\infty \frac{2(M + E)\tilde{\rho}(E)dE}{(E + \Delta)(2M + E - \Delta)}. \quad (68)$$

UV singularities can be removed by subtraction or by dimensional regularization. We again use the unorthodox dimensional regularization prescription. For a general form of the threshold expansion $\tilde{\rho}(E) = E^\gamma \sum a_k E^k$ we have to calculate integrals of the form

$$\tilde{\Pi}^\sigma(\Delta) = \int_0^\infty \frac{E^\sigma dE}{(E + \Delta)(2M + E - \Delta)} = -\frac{\pi}{\sin(\pi\sigma)} \frac{\Delta^\sigma - (2M - \Delta)^\sigma}{2(M - \Delta)}. \quad (69)$$

Only the powers Δ^σ contribute to the singular part of the polarization function. Expressions like the one presented in Eq. (69) then allow one to restore that part of the polarization function $\Pi(p)$ which has singularities near the threshold.

6 Conclusion

We have discussed the configuration space technique for the calculation of n -line two-point diagrams termed water melon diagrams. This technique allows one to calculate the spectral density for arbitrary space-time dimensions and any number of internal lines with arbitrary mass values. Within this technique one can use either an exact representation as one-fold integral or an expansion near the production threshold. We have developed an efficient method for constructing the near threshold expansion of water melon diagrams that uses only asymptotic expansions of Bessel functions which are well-known and simple functions. We have considered a strongly asymmetric mass arrangement where one mass is much smaller than the others. In this case the “pure” threshold expansion which is done in terms of the threshold parameter E breaks down at the energies in the vicinity

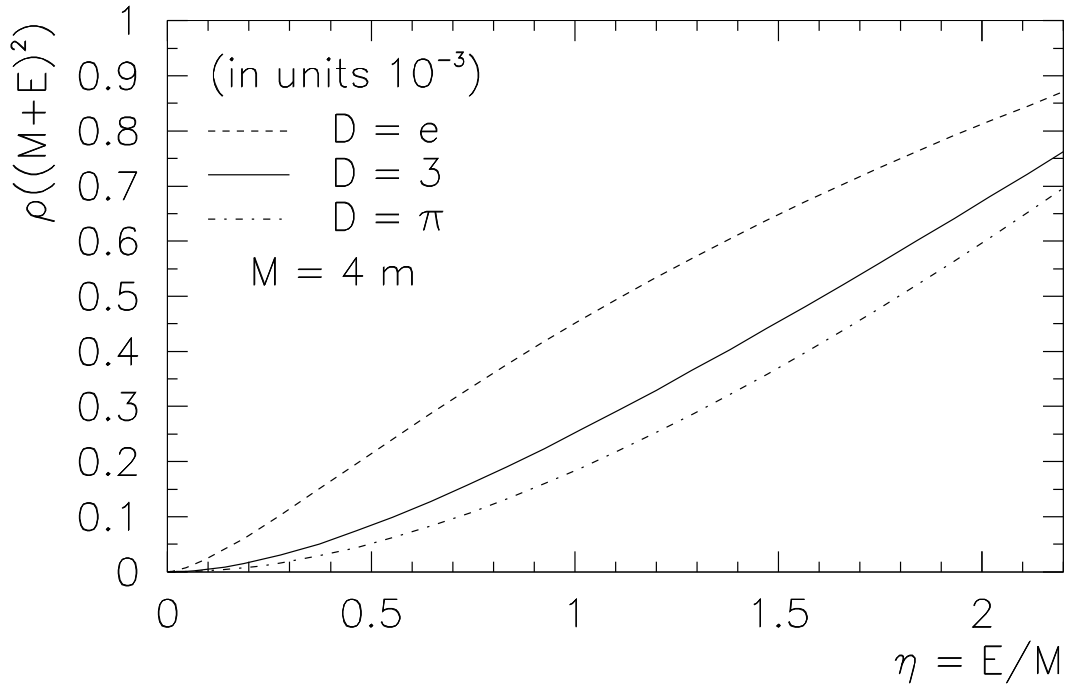


Figure 7: The spectral density for the four-line water melon diagram with equal masses for $D = e = 2.718\dots$, $D = 3$, and $D = \pi = 3.14\dots$ space-time dimensions.

of the smallest mass. In order to extend the approximation to higher energies we have introduced a generalized threshold expansion which exactly resums all contributions of the smallest mass. We have presented closed expressions for the generalized expansion in several particular cases and demonstrated the improvement of the convergence gained by the resummation of the smallest mass contributions. The particular kinematic regime of this case could be treated analytically because it reduced to the evaluation of the one-fold integral in terms of hypergeometric functions. The discontinuity across the physical cut for the generalized expansion has been found in terms of hypergeometric functions as well.

To conclude, we stress that the configuration space technique is a powerful and convenient tool for investigating different properties of water melon diagrams. The practical convenience of our method is demonstrated in Fig. 7 where we have plotted the spectral density for a four-line water melon diagram in $D = e = 2.718\dots$, $D = 3$, and $D = \pi = 3.14\dots$ space-time dimensions.

Acknowledgments

We thank Andrei Davydychev and Jürgen Körner for interesting discussions and careful reading the manuscript. A.A. Pivovarov acknowledges a valuable discussion with V.A. Smirnov on the region separation technique in threshold expansions. The work of A.A. Pivovarov is supported in part by the Volkswagen Foundation under contract No. I/73611 and by the Russian Fund for Basic Research under contract 99-01-00091. S. Groote gratefully acknowledges a grant given by the Graduiertenkolleg “Eichtheorien – experimentelle Tests und theoretische Grundlagen”.

References

- [1] Particle Data Group, “Review of Particle Properties”, Eur. Phys. J. **C3** (1998) 1
- [2] K.G. Chetyrkin, J.H. Kühn and A. Kwiatkowski, Phys. Rep. **277** (1996) 189
- [3] K.G. Chetyrkin, J.H. Kühn and M. Steinhauser, Nucl. Phys. **B505** (1997) 213
- [4] D.J. Broadhurst, Eur. Phys. J. **C8** (1999) 311
- [5] O.M. OGREID, P. OSLAND, “More series related to the Euler series”,
Report No. BERGEN-1999-04, hep-th/9904206
- [6] R. Coquereaux, Phys. Rev. **D23** (1981) 2276;
V.I. Zakharov, Nucl. Phys. **B385** (1992) 452;
D.J. Broadhurst and A.G. Grozin, Phys. Rev. **D52** (1995) 4082
- [7] S. Groote, J.G. Körner and A.A. Pivovarov, Nucl. Phys. **B542** (1999) 515;
Eur. Phys. J. **C11** (1999) 279; Phys. Lett. **443 B** (1998) 269
- [8] F.A. Berends, M. Buza, M. Böhm and R. Scharf, Z. Phys. **C63** (1994) 227

- [9] F.A. Berends, A.I. Davydychev and N.I. Ussyukina,
Phys. Lett. **426 B** (1998) 95
- [10] S. Coleman and E. Weinberg, Phys. Rev. **D7** (1973) 1888;
R. Jackiw, Phys. Rev. **D9** (1974) 1686;
R. Jackiw and S. Templeton, Phys. Rev. **D23** (1981) 2291
- [11] A.K. Rajantie, Nucl. Phys. **B480** (1996) 729
- [12] J.M. Chung and B.K. Chung, “Renormalization group improvement of the effective potential in massive Φ^4 theory: NNNLO logarithm resummation”, Report No. MIT-CTP-2929, hep-th/9911196
- [13] J.O. Andersen, E. Braaten and M. Strickland, “The massive thermal basketball diagram”, hep-ph/0002048
- [14] J.M. Chung and B.K. Chung, Phys. Rev. **D59** (1999) 105014
- [15] D.J. Gross, R.D. Pisarski and L.G. Yaffe, Rev. Mod. Phys. **53** (1981) 43;
T. Appelquist and R.D. Pisarski, Phys. Rev. **D23** (1981) 2305
- [16] B.L. Ioffe, Nucl. Phys. **B188** (1981) 317
- [17] N.V. Krasnikov, A.A. Pivovarov and A.N. Tavkhelidze,
Z. Phys. **C19** (1983) 301; JETP Lett. **36** (1982) 333
- [18] A.A. Ovchinnikov, A.A. Pivovarov and L.R. Surguladze,
Yad. Fiz. **48** (1988) 562; Int. J. Mod. Phys. **A6** (1991) 2025
- [19] S. Groote, J. G. Körner and A. A. Pivovarov, Phys. Rev. **D61** (2000) 071501
- [20] G. 't Hooft, Nucl. Phys. **B72** (1974) 461
- [21] E. Witten, Nucl. Phys. **B160** (1979) 57

- [22] S.A. Larin *et al.*, Yad. Fiz. **44** (1986) 1066
- [23] S.A. Kulagin and A.A. Pivovarov, Yad. Fiz. **45** (1987) 952
- [24] P. Post and K. Schilcher, Phys. Rev. Lett. **79** (1997) 4088
- [25] J. Gasser and M.E. Sainio, Eur. Phys. J. **C6** (1999) 297
- [26] S. Narison and A.A. Pivovarov, Phys. Lett. **327 B** (1994) 341
- [27] I.I. Balitsky, D.I. D’Yakonov and A.V. Yung, Phys. Lett. **112 B** (1982) 71
- [28] D.J. Broadhurst, Z. Phys. **C54** (1992) 599
- [29] P.A. Baikov, “Advanced method of solving recurrence relations for multiloop Feynman integrals”, talk presented at the 6th International Workshop on New Computing Techniques in Physics Research (AIHENP 99), Heraklion, Crete, Greece, 12–16 April, 1999
- [30] N.E. Ligterink, “Solving multiloop Feynman diagrams using light front coordinates”, Report No. ECT-99-016, hep-ph/9911411
- [31] A.I. Davydychev and V.A. Smirnov, Nucl. Phys. **B554** (1999) 391
- [32] B. Kastening, H. Kleinert, “Efficient algorithm for perturbative calculation of multiloop Feynman integrals”, quant-ph/9909017
- [33] G.N. Watson, “Theory of Bessel functions”, Cambridge, 1944
- [34] E. Mendels, Nuovo Cim. **45 A** (1978) 87
- [35] C.S. Meijer, Proc. Amsterdam Akad. Wet. (1940) 599; 702
- [36] A. Erdelyi (Ed.), “Tables of integral transformations”, Volume 2, Bateman manuscript project, 1954

- [37] A.H. Hoang *et al.*, “Top-antitop pair production close to threshold: Synopsis of recent NNLO results,” Report No. SLAC-PUB-8369, hep-ph/0001286;
A. Czarnecky and K. Melnikov, Phys. Rev. Lett. **80** (1998) 2531;
M. Beneke, A. Signer and V.A. Smirnov, Phys. Rev. Lett. **80** (1998) 2535;
K. Melnikov and A. Yelkhovsky, Nucl. Phys. **B528** (1998) 59;
A.A. Penin and A.A. Pivovarov, hep-ph/9904278; Nucl. Phys. **B549** (1999) 217;
Nucl. Phys. **B550** (1999) 375; Phys. Lett. **443 B** (1998) 264;
A.H. Hoang and T. Teubner, Phys. Rev. **D60** (1999) 114027;
T. Nagano, A. Ota and Y. Sumino, Phys. Rev. **D60** (1999) 114014
- [38] N.N. Bogoliubov and D.V. Shirkov, “Quantum fields”, Benjamin, 1983
- [39] A.A. Pivovarov, Phys. Lett. **236 B** (1990) 214; Phys. Lett. **263 B** (1991) 282
- [40] V.A. Smirnov, Phys. Lett. **B404** (1997) 101;
M. Beneke and V.A. Smirnov, Nucl. Phys. **B522** (1998) 321;
V.A. Smirnov and E.R. Rakhmetov, Teor. Mat. Fiz. **120** (1999) 64
- [41] A.P. Prudnikov, Yu.A. Brychkov and O.I. Marichev,
“Integrals and Series”, Vol. 2, Gordon and Breach, New York, 1990
- [42] B.Almgren, Arkiv för Fysik, **38** (1967) 161;
S.Bauberger, F.A. Berends, M. Böhm and M. Buza, Nucl. Phys. **B434** (1995) 383
- [43] S. Groote, J. G. Körner and A. A. Pivovarov, Phys. Rev. **D60** (1999) 061701
- [44] A.A. Pivovarov and V.F. Tokarev, Yad. Fiz. **41** (1985) 524
- [45] I.S. Gradshteyn and I.M. Ryzhik,
“Tables of integrals, series, and products”, Academic Press, 1994
- [46] M. Abramowitz, I.A. Stegun (eds.), “Handbook of Mathematical Functions”, Dover Publ. Inc., New York, 9th Printing, 1970